Sara Cappelli, Amanda Penco[a], Benedetta Mannini, Roberta Cascella, Mark R. Wilson, Heath Ecroyd, Xinyi Li, Joel N. Buxbaum, Christopher M. Dobson, Cristina Cecchi, Annalisa Relini and Fabrizio Chiti*

# Effect of molecular chaperones on aberrant protein oligomers *in vitro*: super-versus sub-stoichiometric chaperone concentrations

DOI 10.1515/hsz-2015-0250
Received September 10, 2015; accepted January 11, 2016

**Abstract:** Living systems protect themselves from aberrant proteins by a network of chaperones. We have tested *in vitro* the effects of different concentrations, ranging from 0 to 16 μM, of two molecular chaperones, namely αB-crystallin and clusterin, and an engineered monomeric variant of transthyretin (M-TTR), on the morphology and cytotoxicity of preformed toxic oligomers of HypF-N, which represent a useful model of misfolded protein aggregates. Using atomic force microscopy imaging and static light scattering analysis, all were found to bind HypF-N oligomers and increase the size of the aggregates, to an extent that correlates with chaperone concentration. SDS-PAGE profiles have shown that the large aggregates were predominantly composed of the HypF-N protein. ANS fluorescence measurements show that the chaperone-induced clustering of HypF-N oligomers does not change the overall solvent exposure of hydrophobic residues on the surface of the oligomers. αB-crystallin, clusterin and M-TTR can diminish the cytotoxic effects of the HypF-N oligomers at all chaperone concentration, as demonstrated by MTT reduction and $Ca^{2+}$ influx measurements. The observation that the protective effect is primarily at all concentrations of chaperones, both when the increase in HypF-N aggregate size is minimal and large, emphasizes the efficiency and versatility of these protein molecules.

**Keywords:** molecular chaperones; protein aggregates; protein homeostasis; protein misfolding.

[a]Present address: Department of Molecular Medicine, University of Pavia, Pavia, Italy and Department of Physics, University of Genoa, Genoa, Italy.
***Corresponding author: Fabrizio Chiti,** Department of Biomedical Experimental and Clinical Sciences, Section of Biochemistry, University of Florence, Viale Morgagni 50, I-50134, Florence, Italy, e-mail: fabrizio.chiti@unifi.it
**Sara Cappelli, Roberta Cascella and Cristina Cecchi:** Department of Biomedical Experimental and Clinical Sciences, Section of Biochemistry, University of Florence, Viale Morgagni 50, I-50134, Florence, Italy
**Amanda Penco and Annalisa Relini:** Department of Physics, University of Genoa, Via Dodecaneso 33, I-16136, Genoa, Italy
**Benedetta Mannini:** Department of Biomedical Experimental and Clinical Sciences, Section of Biochemistry, University of Florence, Viale Morgagni 50, I-50134, Florence, Italy; and Department of Chemistry, University of Cambridge, Lensfiled Road, CB2 1EW Cambridge, UK
**Mark R. Wilson and Heath Ecroyd:** Illawarra Health and Medical Research Institute and School of Biological Sciences, University of Wollongong, Northfields Avenue, Wollongong 2522, NSW, Australia
**Xinyi Li and Joel N. Buxbaum:** Department of Molecular and Experimental Medicine, The Scripps Research Institute, 10550 North Torrey Pines Road, La Jolla, CA 92037, USA
**Christopher M. Dobson:** Department of Chemistry, University of Cambridge, Lensfiled Road, CB2 1EW Cambridge, UK

## Introduction

A large number of pathological conditions arise from the failure of polypeptide chains to adopt or to remain in their native conformational states (Chiti and Dobson, 2006). These conditions are generally described as protein misfolding, or protein conformational diseases and may result in loss of function or a gain of toxic function. Most of these diseases are associated with the conversion of specific proteins from their soluble states into aggregated species that thus become deposited within organs and tissues, either as intracellular inclusions or their deposition as extracellular deposits (Chiti and Dobson, 2006; Rambaran and Serpell, 2008). Molecules with chaperone activity are key components of the quality control processes used by living systems to maintain protein homeostasis in the highly crowded cellular environment. The majority of chaperones are located within cells (Bukau et al., 2006; Hartl et al., 2011), but the presence of protective guardians in the extracellular environment collectively referred to as extracellular chaperones is now widely acknowledged (Wyatt et al., 2012, 2013). Typically, chaperones prevent the aggregation of unfolded polypeptide chains ('holdase' activity) and/

or promote their *de novo* protein folding or refolding, i.e. 'foldase' activity (Hartl et al., 2011; Kim et al., 2013). Some molecular chaperones can also disaggregate protein aggregates (Weibezahn et al., 2005; Hodson et al., 2012; Winkler et al., 2012) or cooperate with proteases to facilitate protein degradation (Pickart and Cohen, 2004; Alexopoulos et al., 2012; Li and Lucius, 2013).

In addition to these functions, chaperones have recently been found to suppress *in vitro* the toxic effects of protein aggregates after the aggregates have formed (Ojha et al., 2011; Mannini et al., 2012; Binger et al., 2013; Cascella et al., 2013a,b). In particular, it has been found for a range of systems that misfolded protein oligomers, incubated with sub-stoichiometric concentrations of chaperones *in vitro*, can be converted into large aggregates with substantially reduced toxicity, in the absence of any significant structural reorganization of the individual molecules within the aggregates (Mannini et al., 2012). It was also found that fibrils formed by apolipoprotein C-II were converted into large fibrillar tangles in the presence of a small heat shock protein (Binger et al., 2013). In a recent report it was found that long-lived *daf-2* mutant *Caenorhabditis elegans* strains were characterized by the accumulation of large chaperone-containing aggregates during aging, relative to age-matched wild-type controls that had a normal lifespan (Walther et al., 2015). This chaperone-driven aggregation process was suggested to neutralize potentially harmful, soluble, oligomeric proteins into innocuous large aggregates. It was found to maintain the proteome in the mutant nematodes, therefore representing an important part of their protein homeostasis system and ability to extend their lifespan (Walther et al., 2015). Hence, it appears that the ability of chaperones to neutralize preformed toxic aggregates is an important feature of the behavior of these molecules, and in the present paper we describe further studies of this phenomenon over a wide range of concentrations both above and below stoichiometric ratios of chaperones to oligomers.

We have tested the effects of different concentrations of two recognized molecular chaperones, namely αB-crystallin (αBc), as an example of an intracellular chaperone, and clusterin (Clu), as an example of an extracellular chaperone, on the toxicity of oligomers formed from the N-terminal domain of HypF protein from *Escherichia coli* (HypF-N). We have also tested on the same aberrant protein oligomers the effect of various concentrations of an engineered monomeric variant of transthyretin (M-TTR) containing two mutations (Phe87Met and Leu110Met) that prevent it from forming normal tetramers (Jiang et al., 2001). Although M-TTR and tetrameric TTR are not generally classified as chaperones, they have been found to act in a chaperone-like manner on a subset of amyloidogenic client proteins: they effectively inhibit the aggregation of the amyloid β peptide (Aβ) associated with Alzheimer's disease and suppress the toxicity of these aggregates and other oligomeric proteins (Li et al., 2011; Cascella et al., 2013a; Li et al., 2013; Buxbaum et al., unpublished). Further, in neurons (but not in liver) TTR has been shown to be regulated by the stress responsive heat shock factor 1 (HSF-1) in parallel with the classical heat shock proteins Hsp40, Hsp70 and Hsp90 (Wang et al., 2014).

We decided to assess the effect of these three proteins on HypF-N oligomers because HypF-N is an amyloidogenic protein and a good model system for a number of reasons. First, it forms fibrils that are morphologically, tinctorially and structurally similar to those found in amyloid deposition diseases (Chiti et al., 2001; Relini et al., 2004). Second, HypF-N forms pre-fibrillar oligomers that are toxic to cells in culture and in animal models (Bucciantini et al., 2002, 2004; Cecchi et al., 2005; Baglioni et al., 2006; Pellistri et al., 2008). Furthermore, HypF-N pre-fibrillar oligomers have similar pathogenic effects as Aβ oligomers on cells at the biochemical, molecular, electrophysiological and animal level (Bucciantini et al., 2004; Tatini et al., 2013). Moreover, under two different solution conditions (conditions A and B, respectively), HypF-N very reproducibly forms two well-characterized types of oligomers with similar morphology but different toxicities (Campioni et al., 2010; Zampagni et al., 2011; Evangelisti et al., 2012; Tatini et al., 2013; Mannini et al., 2014).

In this study we have found that αBc, Clu and M-TTR can promote clustering of the HypF-N type A oligomers into larger species, with sizes that in each case increase linearly with chaperone concentration. We have also observed that concentrations of each of the three chaperones below as well as above stoichiometric ratios relative to HypF-N are sufficient to suppress the toxicity of HypF-N oligomers. Indeed, inhibition of HypF-N oligomer toxicity is also achieved even under conditions when there is minimal increase in oligomer size, demonstrating the efficacy of these species to suppress oligomer toxicity by a variety of mechanisms.

# Results

## HypF-N oligomers are insoluble over a wide range of protein concentration

The formation of HypF-N oligomers was verified by sodium dodecylsulfate polyacrylamide gel electrophoresis

(SDS-PAGE) samples containing oligomeric and native HypF-N at 4 μM concentration (equivalent monomer concentration) were centrifuged in order to separate pellet (P) and supernatant (SN) fractions and these were loaded onto a gel. In the sample containing native HypF-N, the HypF-N band (MW ~10.5 kDa) was observed only in the SN fraction, whereas in the sample containing HypF-N oligomers the HypF-N band was found only in the P fraction (Figure 1A). The larger intensity of the latter band arises from the higher amount of protein loaded onto the electrophoretic gel.

In our prior studies of HypF-N oligomers and chaperones, we used preformed HypF-N oligomers at an equivalent monomer concentration of 12 μM (Mannini et al., 2012; Cascella et al., 2013a), a concentration that is too high for the purpose of studying the effect of a wide range of chaperone concentrations, ranging from sub- to super-stoichiometric, on the morphology and cytotoxicity of HypF-N oligomers. In particular, super-stoichiometric concentrations (i.e. >>12 μM) are too high, due to the difficulties associated with the poor solubility of some chaperones at these concentrations (see below). To choose the range of concentration of HypF-N oligomers optimal for the current investigation, the oligomers were diluted into 20 mM potassium phosphate, pH 7.0, to final concentrations ranging from 0 to 14 μM (monomer concentration) and analyzed using static light scattering (SLS). A linear relationship was found between the concentration of HypF-N oligomers and the intensity of scattered light, suggesting that lower protein concentrations do not induce dissociation of the oligomers and the light scattering intensity is linearly proportional to the concentration of aggregated particles in suspension (Figure 1B). A concentration of 4 μM was therefore chosen as a good compromise to evaluate the effect of both sub-stoichiometric and super-stoichiometric chaperone concentrations on the size and toxicity of HypF-N oligomers.

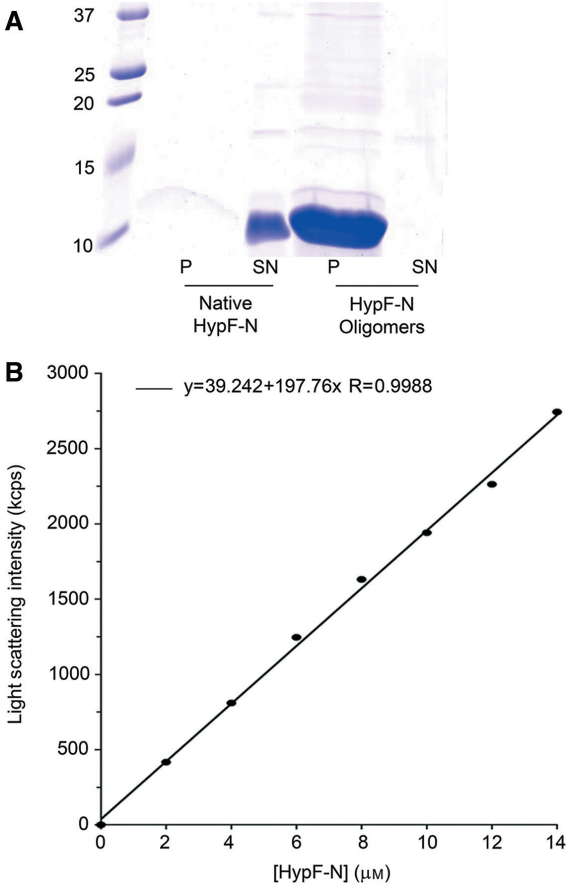


**Figure 1:** Preliminary analysis of HypF-N oligomers.
(A) SDS-PAGE analysis of the pellet (P) and supernatant (SN) fractions obtained from samples containing native HypF-N or HypF-N oligomers through centrifugation. (B) Static light scattering intensity expressed as kilocounts per second (kcps) of HypF-N oligomers at different concentrations. The data can be fit with a straight line, described by the equation in the figure.

## The size of HypF-N oligomers increases with αBc, Clu and M-TTR concentration

To investigate the effects of different concentrations of αBc, Clu and M-TTR on HypF-N aggregate size, we incubated the oligomers (at a concentration equivalent to 4 μM monomer) in the presence of increasing concentrations of each chaperone (0–16 μM) and measured the intensity of scattered light (Figure 2A–C). Relative to the sample containing oligomers alone, the intensity of scattered light was found to increase with the concentration of each chaperone. The increase in light scattering intensity was less marked at low concentrations of each chaperone, but became highly significant at high concentrations.

The soluble chaperones provide a small but significant contribution to light scattering. To exclude the possibility that the observed increase in light scattering intensity coinciding with increases in chaperone concentration solely arose from the chaperones themselves, we performed control experiments using 16 μM αBc, Clu or M-TTR alone, which corresponds to the highest chaperone concentration used in all our experiments. The low values of light scattering intensity observed with 16 μM αBc, Clu and M-TTR alone suggest that the soluble chaperones cannot account for the increase in light scattering intensity observed in the samples containing both oligomers and chaperones (Figure 2).

We also used AFM imaging to determine the morphology and size of HypF-N oligomers in the presence of increasing concentrations of αBc, Clu or M-TTR

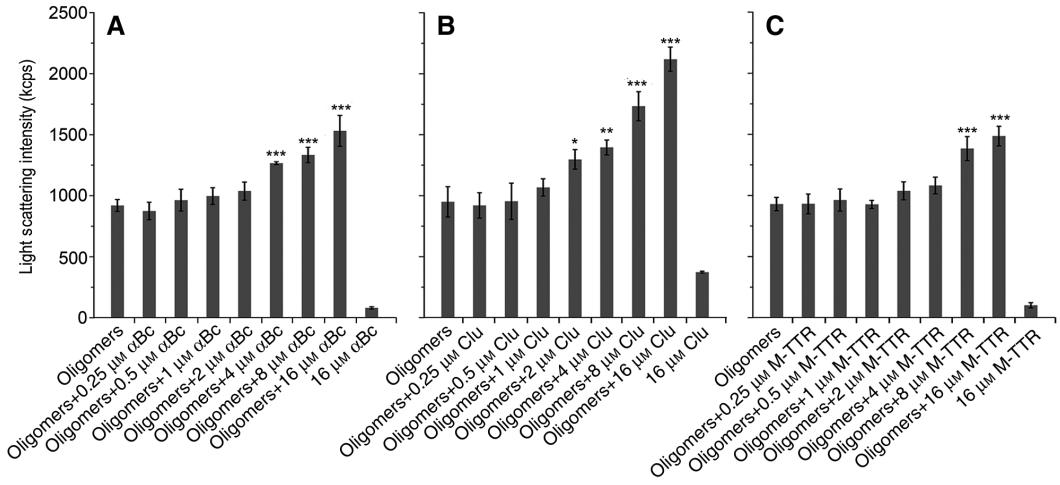


**Figure 2:** Static light scattering intensity measurements (kcps) of HypF-N oligomers (4 μM monomer concentration) incubated with the indicated concentrations of αBc (A), Clu (B) and M-TTR (C). Samples containing 16 μM αBc, Clu or M-TTR are also reported. Error bars correspond to standard errors (SEM) of the means of 4 measurements. The single, double and triple asterisks indicate a significant difference ($p \leq 0.05$, $p \leq 0.01$, $p \leq 0.001$, respectively) relative to the sample containing the oligomers alone.

(Figure 3A–C). In the absence of chaperones the oligomers appear as small spheroids with a height of 2.8±0.2 nm (n=101). This value results from the cross sectional measurements corrected by a shrinking factor of 1.7 and is consistent with that previously reported for HypF-N oligomers (Campioni et al., 2010). In the presence of αBc, Clu and M-TTR at low concentration, we observed aggregates with similar or only slightly higher size. In the presence of the same three proteins at higher concentration, we observed discrete larger aggregates. The largest aggregates were found in samples containing the highest concentration of the chaperones. A quantitative analysis of the sizes of various HypF-N aggregates in the presence of each chaperone showed that both height and width values increase with αBc, Clu and M-TTR concentration (Figure 3D). We did not correct the heights of the aggregates obtained in the presence of chaperones by the shrinking factor in this analysis, as this factor was determined for oligomers alone. Therefore, the aggregate heights reported in Figure 3D should be compared with the uncorrected HypF-N oligomer height, which is 1.66±0.09 nm (n=101). As a control experiment, large aggregates were not observed in samples containing 2.4 μM αBc alone, as reported previously (Mannini et al., 2012).

In conclusion, since the concentration of HypF-N is 4 μM in all cases, the measured increase in aggregate size following the addition of chaperones indicates that the HypF-N oligomers either assemble into larger aggregates in the presence of chaperones or recruit the chaperones themselves into the aggregates.

## The large aggregates primarily contain HypF-N

To determine whether the large aggregates formed in the presence of 4 μM HypF-N and 16 μM αBc, Clu and M-TTR were constituted predominantly of HypF-N, or were complexes of HypF-N and chaperone, we analyzed the samples using SDS-PAGE (Figure 4). In the samples containing HypF-N oligomers alone the HypF-N band (MW ~10.5 kDa) was present only in the P fraction (Figure 4). In the three samples containing only 16 μM αBc, Clu or M-TTR, the αBc band (MW ~20 kDa), the Clu band (MW ~36 kDa) and the M-TTR band (MW ~14 kDa) were found mainly in the SN fraction, although unexpectedly a weak band was also present in the P fraction, suggesting that a very small, yet significant, percentage of each of these proteins were in an aggregated state at these concentrations (Figure 4).

In the samples containing both HypF-N oligomers (4 μM monomer) and 16 μM chaperone the HypF-N band was visible only in the P fraction, whereas the bands representing αBc, Clu and M-TTR were visible in both the P and SN fractions, with the large majority of protein present in the SN fraction (Figure 4). For each of the three chaperones, the band intensity in the P sample containing oligomers and chaperone, determined using densitometry analysis, was weak and only slightly higher than that determined in the P sample containing chaperone alone. This result suggests that the large species observed when HypF-N oligomers were incubated at the highest chaperone concentration did not arise from the recruitment of all available chaperone to the HypF-N oligomers, but rather

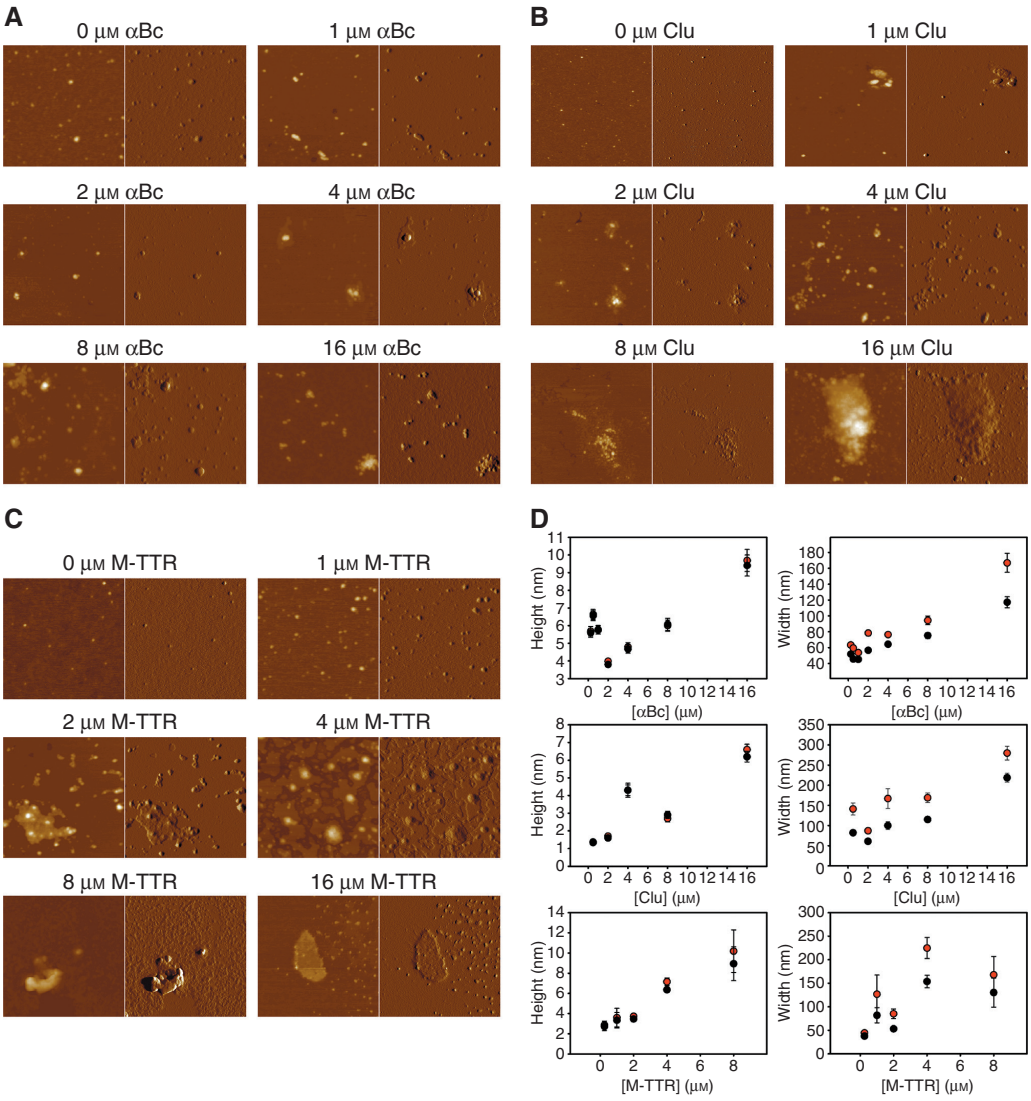


**Figure 3:** AFM analysis of HypF-N oligomers.
(A–C) TM-AFM images (left, height data; right, amplitude data) of HypF-N oligomers (equivalent to 4 μM monomer concentration) pre-incubated with αBc (A), Clu (B), M-TTR (C) at the indicated chaperone concentrations. The scan size is 1.0 μm. The Z range is (with increasing chaperone concentration) 10 nm, 27 nm, 20 nm, 30 nm, 40 nm, 40 nm (A); 6 nm, 40 nm, 8 nm, 18 nm, 10 nm, 35 nm (B); 12 nm, 8 nm, 15 nm, 20 nm, 120 nm, 12 nm (C). (D) The size of HypF-N aggregates in the presence of αBc (top), Clu (middle) or M-TTR (bottom) is measured from the topographic TM-AFM images as the maximum and minimum widths (right panels, red and black circles, respectively) and as the heights evaluated along the sections corresponding to the maximum and minimum widths (left panels, red and black circles, respectively).

from the further assembly of pre-existing HypF-N oligomers induced by a small fraction of chaperone that remains associated with these assemblies.

Overall, the SDS-PAGE results show that (i) each chaperone is significantly insoluble at the concentration of 16 μM, (ii) each chaperone binds HypF-N oligomers only marginally, as the small fraction present in the pellet when both chaperone and oligomers are present results in part from the intrinsic insolubility of a small fraction of the chaperone at this concentration, (iii) the large aggregates observed in the presence of both HypF-N oligomers and chaperone result from the chaperone-induced assembly of HypF-N oligomers into larger species, which appear to consist predominantly of the HypF-N protein.

## αBc, Clu and M-TTR partially aggregate at moderately high concentration

As further evidence that αBc, Clu and M-TTR aggregate at 16 μM concentration, we assessed the size distributions of αBc, Clu and M-TTR alone by light scattering

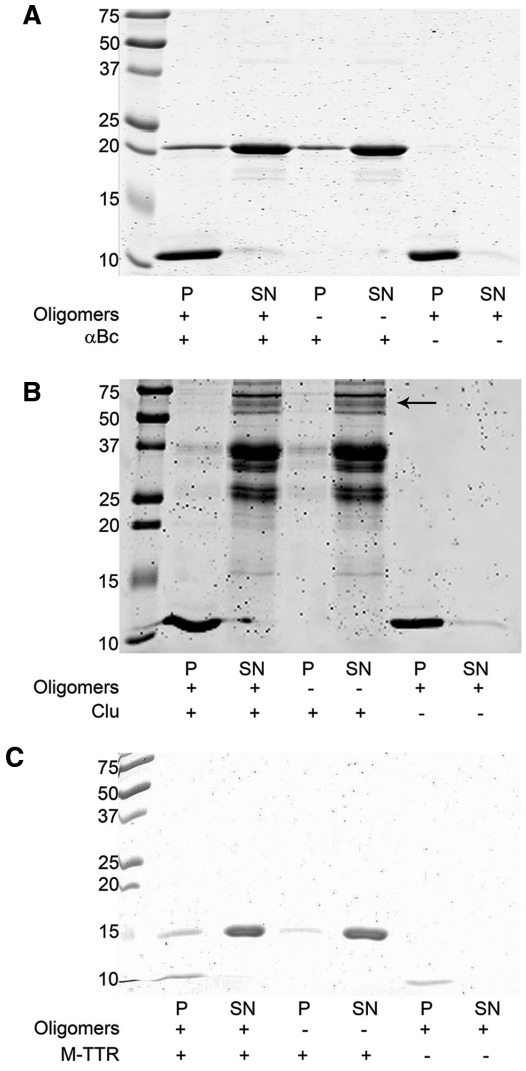


**Figure 4:** SDS-PAGE on samples containing HypF-N oligomers and αBc (A), Clu (B) and M-TTR (C). The samples were prepared by incubating HypF-N oligomers (4 μM monomer) and each chaperone (16 μM) separately or together. They were then centrifuged for 10 min at 16 100 *g* and the P and SN fractions were collected and analyzed by reducing SDS-PAGE. The bands at ~10, ~20, ~36 and ~14 kDa correspond to HypF-N (A–C), αBc (A), Clu (B) and M-TTR (C), respectively. In (B) a lower amount of unprocessed (single chain) and variably glycosylated Clu are also visible at higher molecular weights (black arrow).

(Figure 5). The peak at 18.8±0.4 nm observed in the presence of 16 μM αBc (Figure 5A) is consistent with the hydrodynamic diameter of native αBc (~13.5 nm), as reported previously (Haley et al., 1998; Burgio et al., 2001; Peschek et al., 2009). Indeed, αBc is an oligomer in its native state (Aquilina et al., 2003). In the sample containing Clu, the weak peak at 11.5±0.8 nm (Figure 5B) is consistent with the hydrodynamic diameter of native Clu, as reported previously (Wyatt et al., 2009). This peak is partially masked by species of larger diameter, notably in the ranges of 30–80 nm and 100–600 nm, indicating the presence of a variety of aggregates in solution. Since the intensity of light scattering scales with the square of the particle mass, the predominance of these peaks in the DLS intensity distribution does not indicate that most of Clu is aggregated. Rather, the DLS intensity distribution indicates that most of the Clu adopts a native structure. However, it also provides evidence that aggregates are present. Aggregates were also found in the samples containing M-TTR (Figure 5C), where they completely mask the peak related to the soluble form of M-TTR found at 4.5±0.6 nm (Jiang et al., 2001; Pires et al., 2012; Conti et al., 2014).

The presence of protein aggregates in samples containing 16 μM chaperone was unexpected. We therefore repeated the experiments with Clu at this concentration, but in this case centrifuging and filtering (0.02 μM cutoff) the sample before measuring the DLS distributions at various time points. The aggregates appeared to be present from the start of the experiment, suggesting that they form and equilibrate very rapidly after centrifugation/filtration (data not shown). As all three chaperones were lyophilized after purification and resuspended immediately before the experiments, these aggregates likely originate from the lyophilization and resuspension procedure. We therefore analyzed by DLS a sample of Clu purified from human plasma that had not undergone lyophilization. The DLS distribution indicates that monomeric species are dominant, with only a very small number of aggregates of diameter 30–80 nm and no aggregates with a size larger than 100 nm (Figure 5D).

Overall, the DLS results confirm the data obtained by the SDS-PAGE analysis and suggest that lyophilized/reconstituted αBc, Clu and M-TTR partially assemble into aggregates at the highest concentration studied here. Purified chaperones that have not been subjected to lyophilization and reconstitution do not, however, form significant amounts of these aggregates. Similar behavior has been observed for α-synuclein (Chen et al., 2015).

## Solvent-exposed hydrophobicity of HypF-N oligomers in presence of αBc, Clu and M-TTR

A number of studies indicate that an increase in the exposure of hydrophobic groups on the surface of oligomers positively correlates with their ability to cause cellular dysfunction (Oma et al., 2005; Bolognesi et al., 2010; Olzscha et al., 2011; Ladiwala et al., 2012). This has also been observed for HypF-N oligomers (Campioni et al., 2010; Bemporad and Chiti, 2012). To investigate changes in the extent of exposed hydrophobicity on HypF-N oligomers following

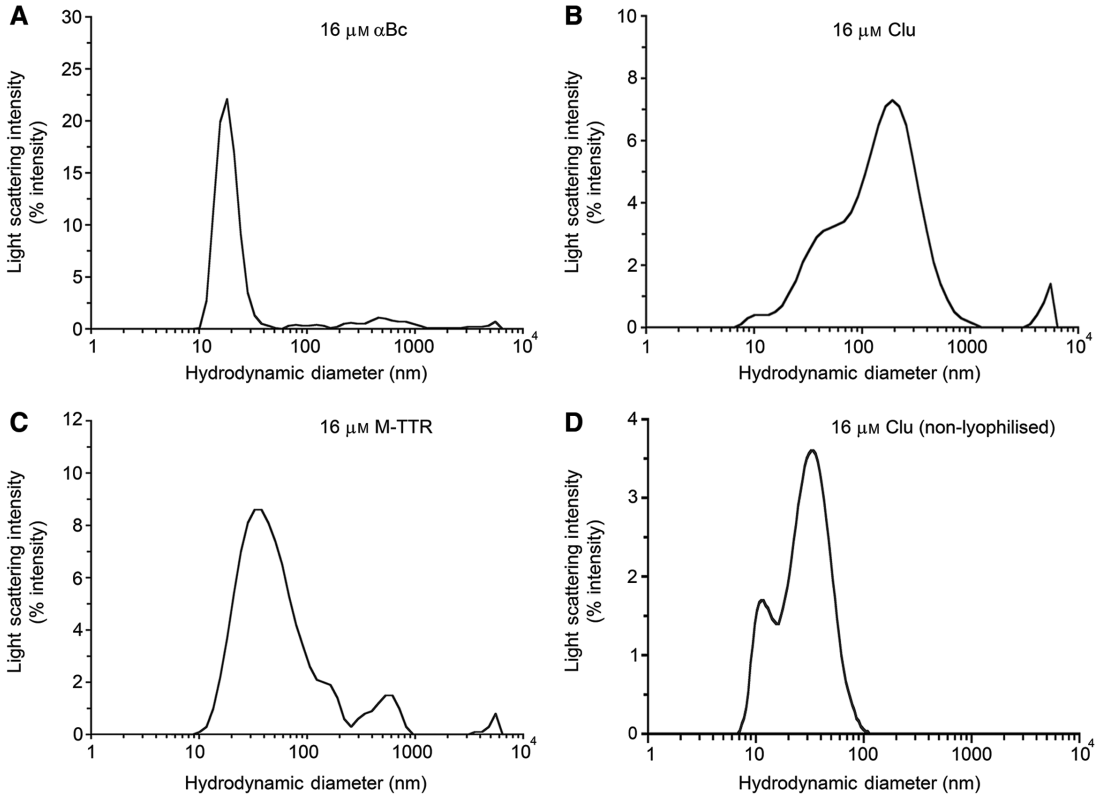


**Figure 5:** DLS analysis of chaperones.
Size distributions by light scattering intensity of αBc (A), Clu (B), M-TTR (C) and Clu before lyophilization (D) at a concentration of 16 μM acquired after incubation of each chaperones for 1 h at 37°C with shaking in 20 mM potassium phosphate pH 7.0.

the addition of chaperones, we measured the fluorescence of ANS in the presence of our samples. ANS is a fluorescent dye that binds to hydrophobic regions on the surface of proteins; this results in an enhanced quantum yield and in a blue shift of the wavelength of maximum emission ($\lambda_{max}$) (Semisotnov et al., 1991; Cardamone and Puri, 1992). The fluorescence spectra of ANS with HypF-N oligomers alone, αBc, Clu or M-TTR alone and HypF-N oligomers in the presence of αBc, Clu or M-TTR were acquired and compared to that of free ANS (Figure 6). The analysis was performed using HypF-N and chaperone concentrations of 48 μM and 9.6 μM, respectively (Figure 6A–C) or 4 μM and 1 μM, respectively (Figure 6D–F). This allowed to observe ANS binding under conditions in which chaperones do (Mannini et al., 2012) or do not promote appreciable clustering of HypF-N oligomers in the first and second cases, respectively.

The binding of ANS to hydrophobic regions exposed on the HypF-N oligomers surface at high concentration (48 μM) results in enhanced quantum yield and in a blue shift of the wavelength of peak emission from 510–530 nm to 470–490 nm. Similar behavior was observed when 9.6 μM αBc and Clu were analyzed separately indicating that these chaperones also have hydrophobic regions exposed on their surface. By contrast, such spectral changes were not observed in the samples containing M-TTR alone, suggesting that this protein, as expected for a fully folded protein, does not present clusters of exposed hydrophobic residues on its surface (Jiang et al., 2001).

For the sample containing both 48 μM oligomers and 9.6 μM chaperone, under conditions in which the chaperone promotes clustering of HypF-N oligomers, the fluorescence spectrum of ANS corresponds to that obtained from a linear combination (sum) of the ANS fluorescence spectra obtained with oligomers alone and chaperone alone (Figure 6A–C). This indicates that the oligomer surface hydrophobicity does not change after the binding of HypF-N oligomers to αBc, Clu or M-TTR under these conditions. By contrast, for the sample containing 4 μM oligomers and 1 μM chaperone, under conditions in which the chaperone does not promote a significant clustering of HypF-N oligomers, the fluorescence spectrum of ANS is lower in intensity than that obtained from a linear combination (sum) of the ANS fluorescence spectra obtained with oligomers alone and chaperone alone at the same concentrations (Figure 6D–F). This indicates that the oligomer surface hydrophobicity is weakly, yet significantly,

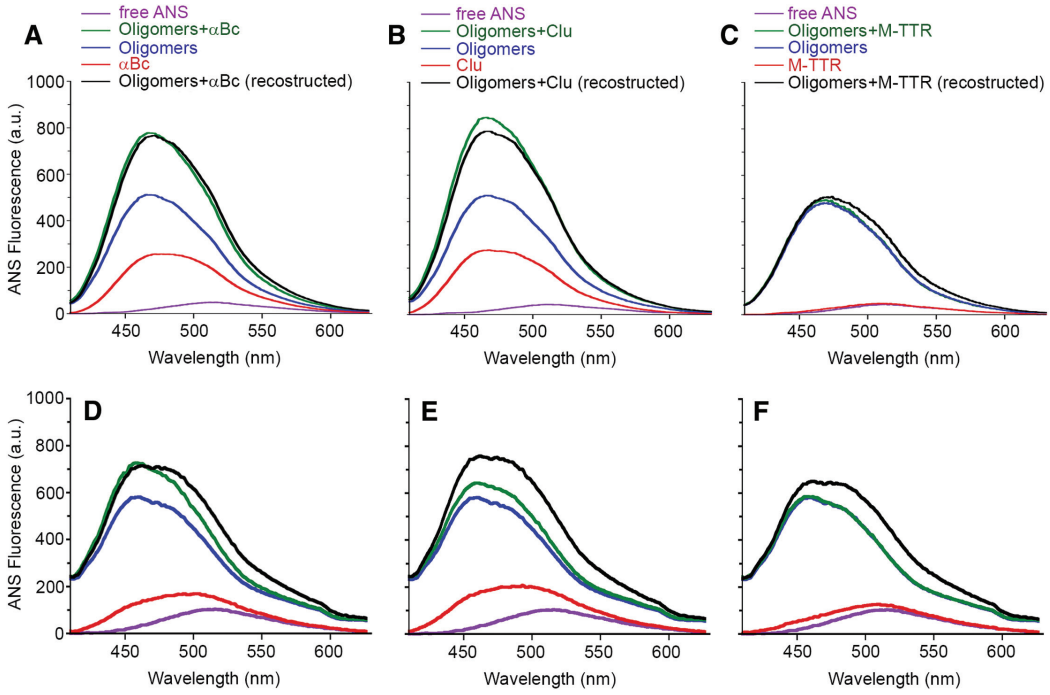


**Figure 6:** ANS analysis of HypF-N oligomers.
ANS fluorescence spectra in the absence of added proteins (purple), in the presence of HypF-N oligomers (blue), chaperone (red) and oligomers and chaperones incubated together (green). The reconstructed spectrum (black) is given by the sum of the spectra of HypF-N oligomers (blue) and chaperone incubated separately (red). The analysis refers to αBc (A,D), Clu (B,E) and M-TTR (C,F) with HypF-N and chaperone concentrations of 48 μM and 9.6 μM (A–C) and 4 μM and 1 μM (D–F), respectively.

shielded after the binding to αBc, Clu or M-TTR under these conditions.

## αBc, Clu and M-TTR inhibit HypF-N oligomer toxicity

The toxicity of HypF-N oligomers and αBc, Clu or M-TTR, preincubated together or separately, were tested using the 3-[4,5-dimethylthiazol-2-yl]-2,5-diphenyltetrazolium bromide (MTT) assay on the murine neuroblastoma N2a cells. When the cells were treated with HypF-N oligomers at a concentration of 4 μM without chaperones, cell viability was found to be 45.5±1.3% with respect to the untreated cells, taken as 100% (Figure 7A–C). In the presence of HypF-N oligomers preincubated with low concentrations of αBc, Clu or M-TTR, cell viability was greater, reaching about 80–85% of the untreated cells, at chaperone concentrations of 0.25 or 0.5 μM (Figure 7A–C). In similar experiments, cell viability decreased at higher chaperone concentrations, down to values of 50–58% at concentrations of 16 μM chaperone. It is important to note, however, that for all chaperone concentrations tested, when HypF-N oligomers were preincubated with chaperone and then added to cells, the level of the toxicity measured was only slightly higher than that for the corresponding concentration of chaperone alone (Figure 7A–C). For example, the measured percent viable cells following incubation with 4 μM HypF-N oligomers preincubated with 16 μM αBc, Clu and M-TTR were 50.7±3.2%, 52.6±2.3%, 57.7±4.0%, respectively, whereas the corresponding values for cells incubated with only 16 μM αBc, Clu and M-TTR were 64.8±1.2%, 57.7±3.6%, 61.8±2.3%, respectively. These data indicate that the toxicity of the HypF-N oligomers is significantly inhibited by the chaperones and that the residual toxicity largely arises from the chaperone itself, probably from the fraction of chaperone in an aggregated form.

To test this possibility, we measured the toxicity of an identical sample of 16 μM Clu that had not undergone lyophilization and resuspension. No detectable toxicity was observed in this case, similarly to a protein sample containing 16 μM BSA, used as a negative control, and unlike a sample containing toxic $NaN_3$, used here as a positive control (Figure 7D). Overall, the results suggest that αBc, Clu and M-TTR inhibit HypF-N oligomer toxicity over the range of concentrations used here. The high levels of toxicity observed when the cells are coincidentally exposed to HypF-N oligomers and high concentrations of αBc, Clu

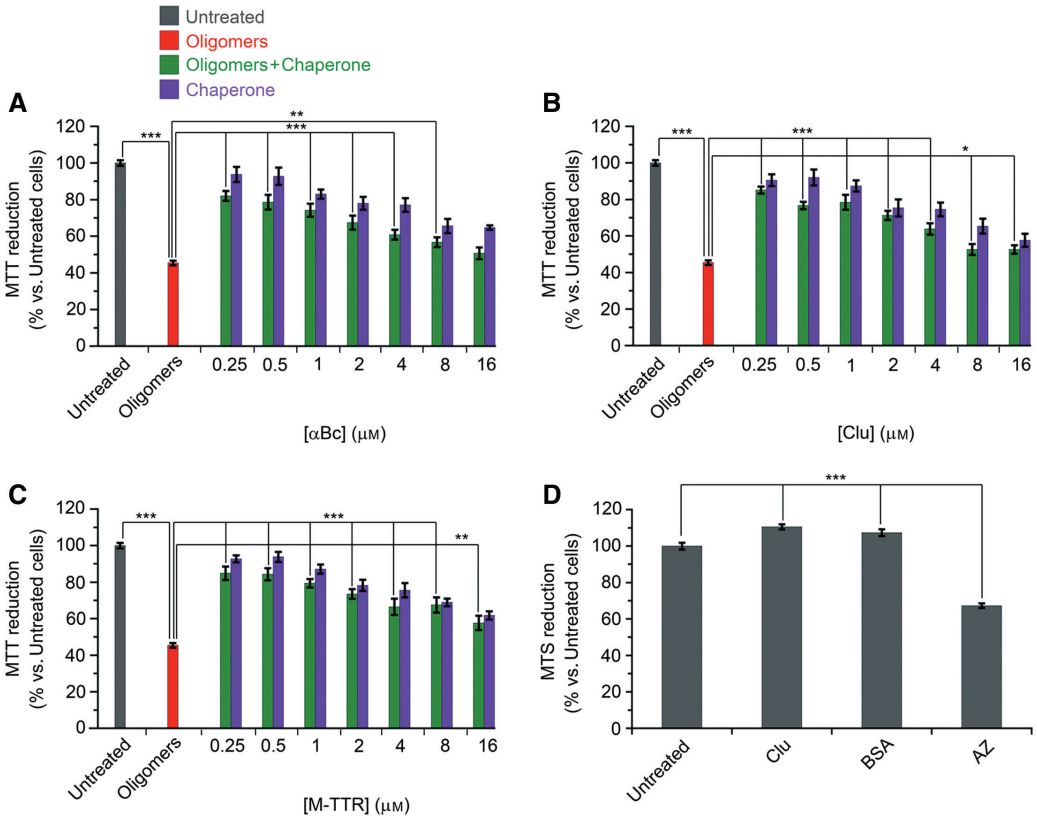


**Figure 7:** Cell viability assay following addition of HypF-N oligomers.
(A–C) MTT reduction assay on N2a cells after treatment with HypF-N oligomers and αBc (A), Clu (B) and M-TTR (C). The HypF-N oligomers (4 μM monomer) and each chaperone at the indicated concentration were incubated for 1 h at 37°C with shaking together or separately and then added to the cells. Each bar in the histogram represents the mean % of MTT reduction ± the standard error of the mean (SEM) of one experiment (n=4). The single, double and triple asterisks indicate significant differences ($p \leq 0.05$, $p \leq 0.01$, $p \leq 0.001$, respectively) between the indicated measurements. (D) MTS assay on N2a cells after treatment with freshly purified Clu, BSA and $NaN_3$ (AZ). Clu and BSA were incubated for 1 h at 37°C with shaking and then added to the cells. Each bar in the histogram represents the mean % of MTS reduction ± the standard error of the mean (SEM) of one experiment (n=8). The triple asterisks indicate significant differences ($p \leq 0.001$) between AZ and the other mesaurements.

or M-TTR likely results from a small fraction of chaperone in an aggregated state, formed after the non-physiological procedure of lyophilization/reconstitution.

An early event arising from the cytotoxicity of protein oligomers is a rapid influx of $Ca^{2+}$ ions from the cell culture medium into the cytosol, attributable to the interaction of the oligomers with the cell membrane (Bucciantini et al., 2004; Demuro et al., 2005, 2011; Zampagni et al., 2011). We tested the effects on N2a cell $Ca^{2+}$ dyshomeostasis of HypF-N oligomers alone, αBc, Clu or M-TTR alone, and HypF-N oligomers incubated with each of these three proteins (Figure 8). The intracellular $Ca^{2+}$-derived fluorescence of cells treated with HypF-N oligomers alone was remarkably high, unlike untreated cells that presented a very weak intracellular fluorescence. The $Ca^{2+}$-derived fluorescence of cells treated with HypF-N oligomers in the presence of αBc, Clu or M-TTR at 1 μM was significantly less evident than that derived from cells treated with HypF-N oligomers alone and more similar to the fluorescence of untreated cells. A similar level of fluorescence was seen when cells were treated with 1 μM αBc, Clu or M-TTR alone. The fluorescence of cells treated with HypF-N oligomers in the presence of 16 μM αBc, Clu or M-TTR was high, but similar to that of cells treated with either of the chaperones at the same concentration. These results confirm those obtained with the MTT assay and together indicate that the toxicity of HypF-N oligomers is inhibited at all concentrations of αBc, Clu or M-TTR investigated here.

# Discussion

## Effects of different concentrations of chaperones

Recently it has been demonstrated that, even when present at very low concentrations, molecular chaperones

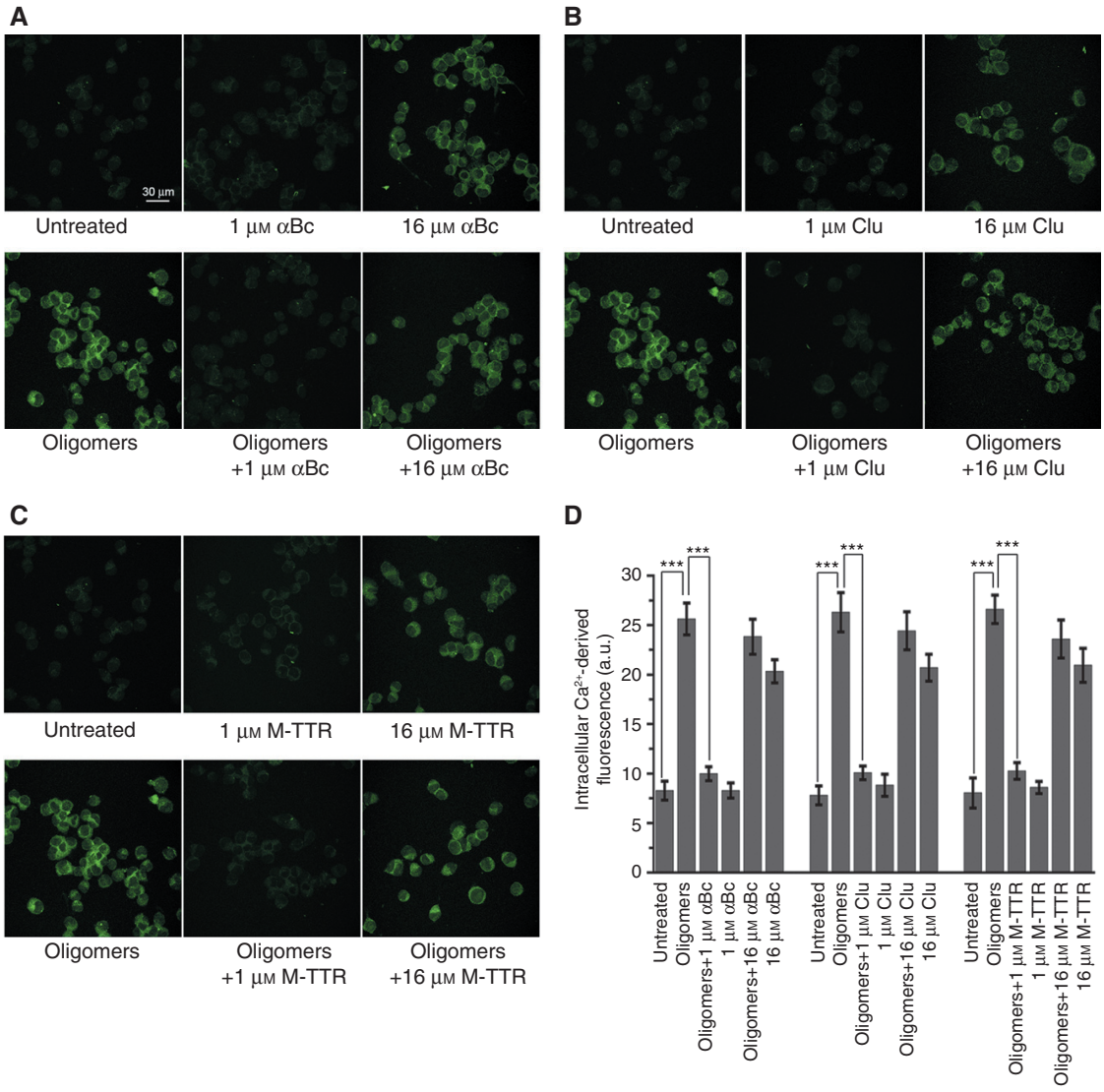


**Figure 8:** Analysis of calcium influx following addition of HypF-N oligomers.
(A–C) Representative confocal scanning microscope images showing intracellular $Ca^{2+}$ levels in N2a cells after treatment with HypF-N oligomers (4 μM monomer) incubated in the absence or in the presence of αBc (A), Clu (B) and M-TTR (C) at the concentration of 1 or 16 μM. Images of the cells treated with chaperones incubated separately at the concentration of 1 and 16 μM were also acquired. The green fluorescence arises from the intracellular Fluo3 probe bound to $Ca^{2+}$. (D) Quantitation of intracellular $Ca^{2+}$-derived fluorescence reported in panels (A)–(C). Each bar reports the mean and SEM (n=4). The triple asterisks indicate significant differences ($p \leq 0.001$) between the indicated measurements.

may inhibit the cytotoxicity of preformed misfolded oligomers formed by Aβ, IAPP and HypF-N and fibrils formed by apolipoprotein C-II, by binding to them and converting them into larger aggregates (Ojha et al., 2011; Mannini et al., 2012, Binger et al., 2013). Interestingly, this chaperone-induced effect has been found to occur in the absence of any major structural reorganization within the individual oligomers, which appear to maintain their overall structure and just assemble into larger species. This effect has also been observed in the presence of tetrameric TTR and, more so, with a variant engineered to be stable as a monomer, M-TTR (Cascella et al., 2013a). Here we found that the size of HypF-N aggregates increases with increasing concentrations of αBc, Clu or M-TTR, as demonstrated by SLS and AFM. The analysis of the protein composition of the aggregates formed in the presence of a molar excess of αBc, Clu or M-TTR through SDS-PAGE revealed that the chaperones bind to the oligomers to only a limited extent. Indeed, most of the chaperone remains in the supernatant, suggesting that these large aggregates arise from the clustering of preexisting HypF-N oligomers, induced by a small fraction of chaperone molecules, rather than the recruitment of all available chaperone molecules to the HypF-N aggregates.

At 4 μM concentration (monomer equivalent) of HypF-N oligomers we have observed inhibition of toxicity over the whole range of chaperone concentrations used in our experiments (0–16 μM), as demonstrated by the MTT reduction assay and $Ca^{2+}$ influx measurements on N2a cells. The SLS and AFM analyses showed that in the presence of the lowest chaperone:HypF-N molar ratio tested here the oligomers maintain a size similar to that observed in their absence but have a significant shielding of their hydrophobic surface, whereas in the presence of the highest molar ratio, the oligomers cluster together reaching a size much higher than that of free oligomers in the absence of a significant hydrophobic shielding. These results indicate that chaperones can inhibit the deleterious biological effects of HypF-N oligomers by binding to their surface without affecting their size, as well as by binding to them and inducing further growth of the aggregated species (Figure 9). In the first case, the chaperones can bind to the hydrophobic groups exposed on the oligomer surface, thus shielding them and preventing them from aberrant interactions with the cells. In the second case, the chaperones can cause a reduction of the surface-volume ratio of the aggregates, decrease the effective concentrations of aggregated particles and decrease their diffusional mobility, as previously suggested (Mannini et al., 2012).

The protective effect mediated by chaperones against misfolded protein oligomers, and observed here in both the presence and absence of their further assembly, allows apparent differences in the proposed mechanisms of action of chaperones to be reconciled. Indeed, the concomitant inhibition of oligomer toxicity and increased oligomer size induced by chaperones, via recruitment of more misfolded protein oligomers into the aggregates, has been interpreted to mean that chaperone-induced clustering of oligomers is a strategy used by chaperones to inhibit oligomer toxicity (Ojha et al., 2011; Mannini et al., 2012, Binger et al., 2013; Cascella et al., 2013a). By contrast, using single-molecule fluorescence techniques, it has been shown that clusterin and αBc are able to bind preformed oligomers of Aβ and sequester them from dissociation or further growth into fibrils, revealing another possible mechanism of action of molecular chaperones which is binding in the absence of aggregate clustering (Narayan et al., 2011, 2012). In the case of Clu, the formation of complexes with misfolded proteins is thought to be relevant in the *in vivo* clearance of these aberrant species via membrane-associated receptors, such as the LRP-2 receptor (Hammad et al., 1997; Cole and Ard, 2000; Bartl et al., 2001).

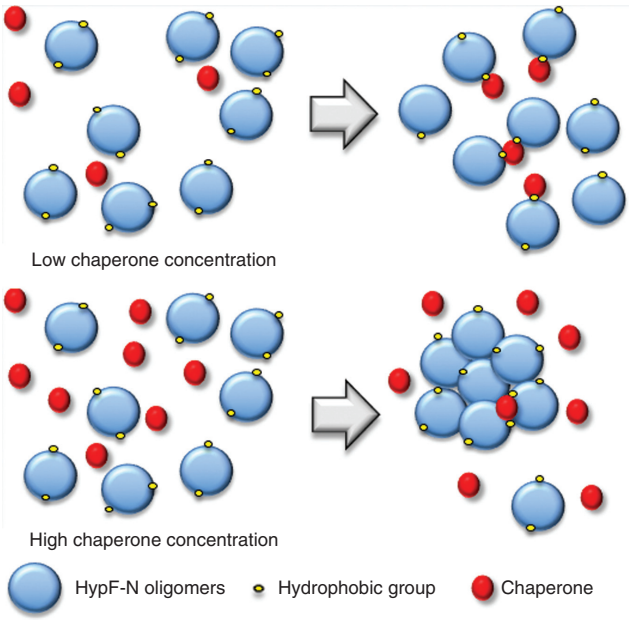


**Figure 9:** A cartoon representing the effect of molecular chaperones at low and high concentration, respectively.

## Comparison with previous studies

Previous reports have shown the effects of molecular chaperones at sub-stoichiometric concentrations (Mannini et al., 2012; Cascella et al., 2013a). Although in previous studies an increase in the size of HypF-N aggregates was evident even at very low concentrations of chaperones (Mannini et al., 2012; Cascella et al., 2013a), the results presented here show that very large increases in aggregate size becomes significant only in the presence of higher chaperone:HypF-N molar ratios. This difference is probably due to the use of different protein concentrations: in the previous studies HypF-N oligomers and chaperones were tested typically at concentrations of 12 μM (equivalent monomer concentration) and 1.2–4.8 μM, respectively, and we observed significant clustering of the HypF-N aggregates. By contrast, the HypF-N oligomers were used here at concentrations of 4 μM (equivalent monomer concentration) and a significant increase of HypF-N oligomer size was observed at chaperone concentrations of 4.0 μM or higher. The lower concentration of HypF-N used here is theoretically expected to shift the equilibrium for the conversion of oligomers and chaperones to chaperone-oligomer complexes (and of the large assemblies of HypF-N) towards the 'reagents', i.e. increasing the population of the small oligomeric species of HypF-N and free chaperones, which is indeed experimentally observed. Consequently, higher concentrations

of chaperones were required in this work to determine a significant increase of HypF-N aggregate size.

Another significant difference between previous and present findings involves the extent of inhibition of HypF-N oligomer toxicity: previous reports showed a complete or nearly complete recovery of cell viability following the pre-incubation of HypF-N oligomers with chaperones (Mannini et al., 2012; Cascella et al., 2013a), whereas the present experiments indicate levels of cell viability that were never higher than 85%, even at low concentrations of chaperone. This lower protective effect may be due to the higher sensitivity of N2a cells used here to measure oligomer toxicity compared to the SH-SY5Y cells used previously, but may also arise from the lower levels of chaperone-induced oligomer clustering reached under our conditions of sub-stoichiometic concentrations of chaperones compared to previous studies (see above), which may render the chaperones less effective in their protective action.

# Conclusions

The protective action of an intracellular chaperone, here αBc, an extracellular chaperone, here Clu, and the extracellular protein with chaperone-like behavior M-TTR, has been evaluated against preformed HypF-N oligomers at different chaperone concentrations. The results show that the size of the HypF-N oligomers increases with chaperone concentration in all three cases and that the aggregates can reach a substantially greater size relative to free HypF-N oligomers with an associated reduction in aggregate toxicity. This protective effect has been observed at all chaperone concentrations tested, emphasizing the efficiency and versatility of these protein molecules, which act to reduce toxicity both by binding to the oligomers without affecting their size and shield their hydrophobic surfaces and also by causing them to further assemble into larger species, with consequent reduction of their surface-volume ratio, effective concentrations of aggregated particles and diffusional mobility.

# Materials and methods

### Formation of HypF-N toxic oligomers

HypF-N was expressed in *E. coli* cells and purified using an affinity chromatography column packed with the HIS-Select Nickel Affinity Gel (Sigma-Aldrich, St. Louis, MO, USA), as previously described (Campioni et al., 2008). The purified native protein was stored at -80°C in 20 mM Tris, 2 mM DTT, pH 8.0 and used as a control (native HypF-N). Toxic oligomers of HypF-N were formed by incubating the native protein at a concentration of 48 μM for 4 h at 25°C in 50 mM acetate buffer, 12% (v/v) trifluoroethanol (TFE), 2 mM DTT, pH 5.5. The oligomers were collected by centrifugation at 16 100 *g* for 10 min, dried under $N_2$, and resuspended in either 20 mM potassium phosphate, pH 7.0 for biophysical/biochemical analysis, or in cell culture medium for cell biology tests. Unless stated otherwise, in all the experiments described below the oligomers were diluted into the same buffer or medium to a final protein concentration of 4 μM (corresponding monomer concentration), incubated for 1 h at 37°C with shaking in the presence of increasing concentrations of chaperones (ranging from 0 to 16 μM) and then subjected to biophysical/biochemical analysis or cell biology assays.

### Preparation of chaperones

Human αBc and M-TTR were purified from *E. coli* expression systems according to previously published protocols (Horwitz et al., 1998; Jiang et al., 2001). Human Clu was purified from plasma as previously reported (Wilson and Easterbrook-Smith, 1992). Lyophilized chaperones were dissolved in water and dialyzed against 20 mM potassium phosphate, pH 7.0, 4°C using a dialysis membrane with a molecular mass cut-off of 3500 Da (Spectrum Laboratories, Los Angeles, CA, USA). Most studies were conducted using liophilized and resuspended chaperones due to the necessity of shipping the samples between collaborating laboratories.

### Light scattering measurements

HypF-N oligomers were first diluted in 20 mM potassium phosphate, pH 7.0, to final concentrations ranging from 0 to 14 μM (corresponding monomer concentration) and then incubated without chaperones for 1 h at 37°C while shaking. In another set of experiments, HypF-N oligomers at a corresponding monomer concentration of 4 μM were incubated for 1 h at 37°C with shaking in 20 mM potassium phosphate, pH 7.0 in the presence of 0 to 16 μM αBc, Clu or M-TTR as described above. As a control, αBc, Clu and M-TTR alone at a concentration of 16 μM were also prepared under the same conditions. Before adding HypF-N oligomers and/or chaperones, all buffer solutions were filtered using filters with a cut-off of 0.02 μm. Light scattering measurements were performed using a Zetasizer Nano S or APS (Malvern, Worcestershire, UK) thermostated with a Peltier temperature controller and using a low volume 3.0×3.0 mm cell or 96-well plate. All the measurements were acquired with fixed parameters (e.g. for the measurements performed on the Nano S the cell position 4.20 mm, attenuator index 10) at 37°C.

### Tapping mode atomic force microscopy (TM-AFM)

HypF-N oligomers were incubated in the presence of each chaperone as described above. Samples containing HypF-N oligomers incubated in isolation and in combination of increasing concentrations of each chaperone were then diluted 100-fold; 10 μl aliquots of the diluted samples were deposited on freshly cleaved mica and dried under mild vacuum. Tapping mode AFM images were acquired in air using a Multimode SPM, equipped with 'E' scanning head (maximum scan size 10 μm) and driven by a Nanoscope V controller, and a Dimension 3100 SPM, equipped with a 'G' scanning head (maximum

scan size 100 μm) and driven by a Nanoscope IIIa controller (Digital Instruments, Bruker AXS GmbH, Karlsruhe, Germany). Single beam uncoated silicon cantilevers (type OMCL-AC160TS, Olympus, Tokyo, Japan) were used. The drive frequency was 290–340 kHz and the scan rate was 0.3–0.8 Hz. Aggregate sizes were estimated from heights and widths in cross section of the topographic AFM images. For aggregates obtained in the presence of chaperones, to take into account possible asymmetries in the aggregate shape, we considered both the maximum and minimum widths and the corresponding heights evaluated along the same image sections.

### SDS-PAGE

Oligomers of HypF-N (4 μM monomer equivalent concentration) were incubated with 16 μM αBc, Clu or M-TTR as described above. In control experiments oligomers alone and each chaperone alone were also incubated under the same conditions. Samples were then centrifuged for 10 min at 16 100 *g* and the pellet (P) and supernatant (SN) fractions were subjected to sodium dodecylsulfate polyacrylamide gel electrophoresis (SDS-PAGE) analysis using 15% (w/v) polyacrylamide gels. Proteins were visualized by Coomassie Blue staining. In other experiments, samples containing native HypF-N and HypF-N oligomers were centrifuged for 10 min at 16 100 *g* and the P and SN fractions were analyzed by SDS-PAGE.

### ANS fluorescence

HypF-N oligomers (48 μM or 4 μM monomer concentration) were incubated with 9.6 μM or 1 μM αBc, Clu or M-TTR, for 1 h at 37°C while shaking. Oligomers and each chaperone were also incubated separately under the same conditions. Aliquots of ANS dissolved in 20 mM potassium phosphate, pH 7.0 were added to the oligomers in order to obtain a final 3:1 molar excess of dye. Samples with the same final ANS concentration and without HypF-N/chaperones were also prepared as controls. Fluorescence spectra were acquired using a LS 55 spectrofluorometer (Perkin-Elmer, Waltham, MA, USA) equipped with a thermostated cell holder attached to a Thermo Haake C25P water bath (Karlsruhe, Germany) at 37°C and using a 10×2 mm quartz cell. The excitation wavelength was 380 nm.

### Cell cultures

Murine Neuro2a (N2a) neuroblastoma cells (A.T.C.C., Manassas, VA, USA) were cultured in minimum essential medium eagle (MEM) supplemented with 10% (v/v) fetal bovine serum (FBS), 1 mM glutamine and antibiotics (Sigma-Aldrich, St. Louis, MO, USA). Cell cultures were maintained in a 5% $CO_2$ humidified atmosphere at 37°C and grown until 80% confluence for a maximum of 20 passages.

### MTT and MTS assays

Cells were treated for 24 h with HypF-N oligomers (4 μM monomer) and chaperones (0–16 μM) pre-incubated in combination or in isolation for 1 h at 37°C with shaking in cell culture medium. The MTT reduction assay was performed on N2A cell cultures as previously described (Campioni et al., 2010). In another experiment, N2a cells were seeded into the wells of a sterile 96-well plate to approximately 30% confluence; the growth medium was 90 μl/well of 10% (v/v) FCS in DMEM:F12 (both from Trace Biosciences, Melbourne, Australia) containing penicillin/streptomycin. The following day, solutions of freshly purified Clu and BSA in PBS were gently incubated at 37°C for 1 h on an orbital shaker, and then added into quadruplicate wells to give a final concentration of ca. 1 mg/ml (i.e. 16 μM). The control wells received either no additions or 0.1% $NaN_3$. The cultures were subsequently incubated overnight at 37°C and 5% (v/v) $CO_2$, before performing a CellTiter 96 Aqueous One Solution Cell Proliferation (MTS) assay according to the manufacturer's instructions (Promega, Fitchburg, WI, USA).

### Measurement of intracellular $Ca^{2+}$ levels

Oligomers of HypF-N (4 μM monomer) were incubated for 1 h at 37°C with shaking in cell culture medium with or without 1 μM or 16 μM of αBc, Clu, or M-TTR and then added to N2a cells seeded on glass coverslips for 60 min at 37°C. Cells were then loaded for 30 min with 4.4 μM fluo3-AM (Life Technologies, Carlsbad, CA, USA) with 0.01% (w/v) pluronic acid F-127 (Sigma-Aldrich, St. Louis, MO, USA) in culture medium at 37°C. The cells were then washed with PBS and fixed for 10 min at room temperature with 2% (v/v) paraformaldehyde (Sigma-Aldrich, St. Louis, MO, USA) in PBS. Finally, the paraformaldehyde solution was removed and the coverslips were washed with PBS and water to be mounted on slides for the confocal microscopy analysis. Cell fluorescence was analyzed by a Leica TCS SP5 confocal scanning microscope (Leica Microsystems, Mannheim, Germany), as previously described (Campioni et al., 2010; Zampagni et al., 2011).

### Statistical analysis

Data was expressed as mean±standard error of the mean (SEM). Comparisons between group pairs were performed using the Student's t test. A *p*-value lower than 0.05 was considered statistically significant.

**Acknowledgments:** This work was supported with the 'Fondi di Ateneo' of the University of Florence, Italy.

## References

Alexopoulos, J.A., Guarné, A., and Ortega, J. (2012). ClpP: a structurally dynamic protease regulated by AAA+ proteins. J. Struct. Biol. *179*, 202–210.

Aquilina, J.A., Benesch, J.L., Bateman, O.A., Slingsby, C., and Robinson, C.V. (2003). Polydispersity of a mammalian chaperone: mass spectrometry reveals the population of oligomers in alphaB-crystallin. Proc. Natl. Acad. Sci. USA *100*, 10611–10616.

Baglioni, S., Casamenti, F., Bucciantini, M., Luheshi, L.M., Taddei, N., Chiti, F., Dobson, C.M., and Stefani, M. (2006).

Prefibrillar amyloid aggregates could be generic toxins in higher organisms. J. Neurosci. *26*, 8160–8167.

Bartl, M.M., Luckenbach, T., Bergner, O., Ullrich, O., and Koch-Brandt, C. (2001). Multiple receptors mediate apoJ-dependent clearance of cellular debris into nonprofessional phagocytes. Exp. Cell. Res. *271*, 130–141.

Bemporad, F. and Chiti, F. (2012). Protein misfolded oligomers: experimental approaches, mechanism of formation, and structure-toxicity relationships. Chem. Biol. *19*, 315–327.

Binger, K.J., Ecroyd, H., Yang, S., Carver, J.A., Howlett, G.J., and Griffin, M.D. (2013). Avoiding the oligomeric state: αB-crystallin inhibits fragmentation and induces dissociation of apolipoprotein C-II amyloid fibrils. FASEB J. *27*, 1214–1222.

Bolognesi, B., Kumita, J.R., Barros, T.P., Esbjorner, E.K., Luheshi, L.M., Crowther, D.C., Wilson, M.R., Dobson, C.M., Favrin, G., and Yerbury, J.J. (2010). ANS binding reveals common features of cytotoxic amyloid species. ACS Chem. Biol. *5*, 735–740.

Bucciantini, M., Giannoni, E., Chiti, F., Baroni, F., Formigli, L., Zurdo, J., Taddei, N., Ramponi, G., Dobson, C.M., and Stefani, M. (2002). Inherent toxicity of aggregates implies a common mechanism for protein misfolding diseases. Nature *416*, 507–511.

Bucciantini, M., Calloni, G., Chiti, F., Formigli, L., Nosi, D., Dobson, C.M., and Stefani, M. (2004). Prefibrillar amyloid protein aggregates share common features of cytotoxicity. J. Biol. Chem. *279*, 31374–31382.

Bukau, B., Weissman, J., and Horwich, A. (2006). Molecular chaperones and protein quality control. Cell *125*, 443–451.

Burgio, M.R., Bennett, P.M., and Koretz, J.F. (2001). Heat-induced quaternary transitions in hetero- and homo-polymers of α-crystallin. Mol. Vis. *7*, 228–233.

Campioni, S., Mossuto, M.F., Torrassa, S., Calloni, G., de Laureto, P.P., Relini, A., Fontana, A., and Chiti, F. (2008). Conformational properties of the aggregation precursor state of HypF-N. J. Mol. Biol. *379*, 554–567.

Campioni, S., Mannini, B., Zampagni, M., Pensalfini, A., Parrini, C., Evangelisti, E., Relini, A., Stefani, M., Dobson, C.M., Cecchi, C. et al. (2010). A causative link between the structure of aberrant protein oligomers and their toxicity. Nat. Chem. Biol. *6*, 140–147.

Cardamone, M. and Puri, N.K. (1992). Spectrofluorimetric assessment of the surface hydrophobicity of proteins. Biochem. J. *282*, 589–593.

Cascella, R., Conti, S., Mannini, B., Li, X., Buxbaum, J.N., Tiribilli, B., Chiti, F., and Cecchi, C. (2013a). Transthyretin suppresses the toxicity of oligomers formed by misfolded proteins in vitro. Biochim. Biophys. Acta *1832*, 2302–2314.

Cascella, R., Conti, S., Tatini, F., Evangelisti E., Scartabelli, T., Casamenti, F., Wilson, M.R., Chiti, F., and Cecchi, C. (2013b). Extracellular chaperones prevent Aβ(42)-induced toxicity in rat brains. Biochim. Biophys. Acta *1832*, 1217–1226.

Cecchi, C., Baglioni, S., Fiorillo, C., Pensalfini, A., Liguri, G., Nosi, D., Rigacci, S., Bucciantini, M., and Stefani, M. (2005). Insights into the molecular basis of the differing susceptibility of varying cell types to the toxicity of amyloid aggregates. J. Cell. Sci. *118*, 3459–3470.

Chen, S.W., Drakulic, S., Deas, E., Ouberai, M., Aprile, F.A., Arranz, R., Ness, S., Roodveldt, C., Guilliams, T., De-Genst, E.J., et al. (2015). Structural characterization of toxic oligomers that are kinetically trapped during α-synuclein fibril formation. Proc. Natl. Acad. Sci. USA *112*, E1994–2003.

Chiti, F. and Dobson, C.M. (2006). Protein misfolding, functional amyloid, and human disease. Annu. Rev. Biochem. *75*, 333–366.

Chiti, F., Bucciantini, M., Capanni, C., Taddei, N., Dobson, C.M., and Stefani, M. (2001). Solution conditions can promote formation of either amyloid protofilaments or mature fibrils from the HypF N-terminal domain. Protein Sci. 10, 2541–2547.

Cole, G.M. and Ard, M.D. (2000). Influence of lipoproteins on microglial degradation of Alzheimer's amyloid β-protein. Microsc. Res. Tech. *50*, 316–324.

Conti, S., Li, X., Gianni, S., Ghadami, S.A., Buxbaum, J., Cecchi, C., Chiti, F., and Bemporad, F. (2014). A complex equilibrium among partially unfolded conformations in monomeric transthyretin. Biochemistry *53*, 4381–4392.

Demuro, A., Mina, E., Kayed, R., Milton, S.C., Parker, I., and Glabe, C.G. (2005). Calcium dysregulation and membrane disruption as a ubiquitous neurotoxic mechanism of soluble amyloid oligomers. J. Biol. Chem. *280*, 17294–17300.

Demuro, A., Smith, M., and Parker, I. (2011). Single-channel $Ca^{2+}$ imaging implicates Aβ1-42 amyloid pores in Alzheimer's disease pathology. J. Cell Biol. *195*, 515–524.

Evangelisti, E., Cecchi, C., Cascella, R., Sgromo, C., Becatti, M., Dobson, C.M., Chiti, F., and Stefani, M. (2012). Membrane lipid composition and its physicochemical properties define cell vulnerability to aberrant protein oligomers. J. Cell. Sci. *125*, 2416–2427.

Haley, D.A., Horwitz, J., and Stewart, P.L. (1998). The small heat-shock protein, αB-crystallin, has a variable quaternary structure. J. Mol. Biol. *277*, 27–35.

Hammad, S.M., Ranganathan, S., Loukinova, E., Twal, W.O., and Argraves, W.S. (1997). Interaction of apolipoprotein J-amyloid beta-peptide complex with low density lipoprotein receptor-related protein-2/megalin. A mechanism to prevent pathological accumulation of amyloid β-peptide. J. Biol. Chem. *272*, 18644–18649.

Hartl, F.U., Bracher, A., and Hayer-Hartl, M. (2011). Molecular chaperones in protein folding and proteostasis. Nature *475*, 324–332.

Hodson, S., Marshall, J.J., and Burston, S.G. (2012). Mapping the road to recovery: the ClpB/Hsp104 molecular chaperone. J. Struct. Biol. *179*, 161–171.

Horwitz, J., Huang, Q.L., Ding, L., and Bova, M.P. (1998). Lens α-crystallin: chaperone-like properties. Meth. Enzymol. *290*, 365–383.

Jiang, X., Smith, C.S., Petrassi, H.M., Hammarström, P., White, J.T., Sacchettini, J.C., and Kelly, J.W. (2001). An engineered transthyretin monomer that is nonamyloidogenic, unless it is partially denatured. Biochemistry *40*, 11442–11452.

Kim, Y.E., Hipp, M.S., Bracher, A., Hayer-Hartl, M., and Hartl, F.U. (2013). Molecular chaperone functions in protein folding and proteostasis. Annu. Rev. Biochem. *82*, 323–355.

Ladiwala, A.R., Litt, J., Kane, R.S., Aucoin, D.S., Smith, S.O., Ranjan, S., Davis, J., Van Nostrand, W.E., and Tessier, P.M. (2012). Conformational differences between two amyloid β oligomers of similar size and dissimilar toxicity. J. Biol. Chem. *287*, 24765–24773.

Li, T. and Lucius, A.L. (2013). Examination of the polypeptide substrate specificity for *Escherichia coli* ClpA. Biochemistry *52*, 4941–4954.

Li, X., Masliah, E., Reixach, N., and Buxbaum, J.N. (2011). Neuronal production of transthyretin in human and murine Alzheimer's disease: is it protective? J. Neurosci. *31*, 12483–12490.

Li, X., Zhang, X., Ladiwala, A.R., Du, D., Yadav, J.K., Tessier, P.M., Wright, P.E., Kelly, J.W., and Buxbaum, J.N. (2013). Mechanisms of transthyretin inhibition of β-amyloid aggregation *in vitro*. J. Neurosci. *33*, 19423–19433.

Mannini, B., Cascella, R., Zampagni, M., van Waarde-Verhagen, M., Meehan, S., Roodveldt, C., Campioni, S., Boninsegna, M., Penco, A., Relini, A., et al. (2012). Molecular mechanisms used by chaperones to reduce the toxicity of aberrant protein oligomers. Proc. Natl. Acad. Sci. USA *109*, 12479–12484.

Mannini, B., Mulvihill, E., Sgromo, C., Cascella, R., Khodarahmi, R., Ramazzotti, M., Dobson, C.M., Cecchi, C., and Chiti, F. (2014). Toxicity of protein oligomers is rationalized by a function combining size and surface hydrophobicity. ACS Chem. Biol. *9*, 2309–2317.

Narayan, P., Orte, A., Clarke, R.W., Bolognesi, B., Hook, S., Ganzinger, K.A., Meehan, S., Wilson, M.R., Dobson, C.M., and Klenerman, D. (2011). The extracellular chaperone clusterin sequesters oligomeric forms of the amyloid-β (1-40) peptide. Nat. Struct. Mol. Biol. *19*, 79–83.

Narayan, P., Meehan, S., Carver, J.A., Wilson, M.R., Dobson, C.M., and Klenerman, D. (2012). Amyloid-β oligomers are sequestered by both intracellular and extracellular chaperones. Biochemistry *51*, 9270–9276.

Ojha, J., Masilamoni, G., Dunlap, D., Udoff, R.A., and Cashikar, A.G. (2011). Sequestration of toxic oligomers by HspB1 as a cytoprotective mechanism. Mol. Cell. Biol. *31*, 3146–3157.

Olzscha, H., Schermann, S.M., Woerner, A.C., Pinkert, S., Hecht, M.H., Tartaglia, G.G., Vendruscolo, M., Hayer-Hartl, M., Hartl, F.U., and Vabulas, R.M. (2011). Amyloid-like aggregates sequester numerous metastable proteins with essential cellular functions. Cell *144*, 67–78.

Oma, Y., Kino, Y., Sasagawa, N., and Ishiura, S. (2005). Comparative analysis of the cytotoxicity of homopolymeric amino acids. Biochim. Biophys. Acta *1748*,174–179.

Pellistri, F., Bucciantini, M., Relini, A., Nosi, D., Gliozzi, A., Robello, M., and Stefani, M. (2008). Nonspecific interaction of prefibrillar amyloid aggregates with glutamatergic receptors results in $Ca^{2+}$ increase in primary neuronal cells. J. Biol. Chem. *283*, 29950–29960.

Peschek, J., Braun, N., Franzmann, T.M., Georgalis, Y., Haslbeck, M., Weinkauf, S., and Buchner, J. (2009). The eye lens chaperone α-crystallin forms defined globular assemblies. Proc. Natl. Acad. Sci. USA *106*, 13272–13277.

Pickart, C.M. and Cohen, R.E. (2004). Proteasomes and their kin: proteases in the machine age. Nat. Rev. Mol. Cell. Biol. *5*, 177–187.

Pires, R.H., Karsai, Á., Saraiva, M.J., Damas, A.M., and Kellermayer, M.S. (2012). Distinct annular oligomers captured along the assembly and disassembly pathways of transthyretin amyloid protofibrils. PLoS One *7*, e44992.

Rambaran, R.N. and Serpell, L.C. (2008). Amyloid fibrils: abnormal protein assembly. Prion *2*, 112–117.

Relini, A., Torrassa, S., Rolandi, R., Gliozzi, A., Rosano, C., Canale, C., Bolognesi, M., Plakoutsi, G., Bucciantini, M., Chiti, F., et al. (2004). Monitoring the process of HypF fibrillization and liposome permeabilization by protofibrils. J. Mol. Biol. *338*, 943–957.

Semisotnov, G.V., Rodionova, N.A., Razgulyaev, O.I., Uversky, V.N., Gripas', A.F., and Gilmanshin, R.I. (1991). Study of the "molten globule" intermediate state in protein folding by a hydrophobic fluorescent probe. Biopolymers *31*, 119–128.

Tatini, F., Pugliese, A.M., Traini, C., Niccoli, S., Maraula, G., Ed Dami, T., Mannini, B., Scartabelli, T., Pedata, F., Casamenti, F., et al. (2013). Amyloid-β oligomer synaptotoxicity is mimicked by oligomers of the model protein HypF-N. Neurobiol. Aging. *34*, 2100–2109.

Walther, D.M., Kasturi, P., Zheng, M., Pinkert, S., Vecchi, G., Ciryam, P., Morimoto, R.I., Dobson, C.M., Vendruscolo, M., Mann, M., et al. (2015). Widespread proteome remodeling and aggregation in aging *C. elegans*. Cell *161*, 919–932.

Wang, X., Cattaneo, F., Ryno, L., Hulleman J., Reixach N., and Buxbaum, J.N. (2014) The systemic amyloid precursor transthyretin (TTR) behaves as a neuronal stress protein regulated by HSF1 in SH-SY5Y human neuroblastoma cells and APP23 Alzheimer's disease model mice. J. Neurosci. *34*, 7253–7265.

Weibezahn, J., Schlieker, C., Tessarz, P., Mogk, A., and Bukau, B. (2005). Novel insights into the mechanism of chaperone-assisted protein disaggregation. Biol. Chem. *386*, 739–744.

Wilson, M.R. and Easterbrook-Smith, S.B. (1992). Clusterin binds by a multivalent mechanism to the Fc and Fab regions of IgG. Biochim. Biophys. Acta *1159*, 319–326.

Winkler, J., Tyedmers, J., Bukau, B., and Mogk, A. (2012). Chaperone networks in protein disaggregation and prion propagation. J. Struct. Biol. *179*, 152–160.

Wyatt, A.R., Yerbury, J.J., and Wilson, M.R. (2009). Structural characterization of clusterin-client protein complexes. J. Biol. Chem. *284*, 21920–21927.

Wyatt, A.R., Yerbury, J.J., Dabbs, R.A., and Wilson, M.R. (2012). Roles of extracellular chaperones in amyloidosis. J. Mol. Biol. *421*, 499–516.

Wyatt, A.R., Yerbury, J.J., Ecroyd, H., and Wilson, M.R. (2013). Extracellular chaperones and proteostasis. Annu. Rev. Biochem. *82*, 295–322.

Zampagni, M., Cascella, R., Casamenti, F., Grossi, C., Evangelisti, E., Wright, D., Becatti, M., Liguri, G., Mannini, B., Campioni, S., et al. (2011). A comparison of the biochemical modifications caused by toxic and non-toxic protein oligomers in cells. J. Cell. Mol. Med. *15*, 2106–2116.